Simultaneous valence shift of Pr and Tb ions at the spin-state transition in $(Pr_{1-y}Tb_y)_{0.7}Ca_{0.3}CoO_3$

H. Fujishiro,[1] T. Naito,[1] D. Takeda,[1] N. Yoshida,[1] T. Watanabe,[1] K. Nitta,[2] J. Hejtmánek,[3] K. Knížek,[3] and Z. Jirák[3]

[1]*Faculty of Engineering, Iwate University, 4-3-5 Ueda, Morioka 020-8551, Japan*

[2]*Japan Synchrotron Radiation Research Institute, Sayo, Hyogo 679-5198, Japan*

[3]*Institute of Physics, ASCR, Cukrovarnická 10, 162 00 Prague 6, Czech Republic*

(Received 11 December 2012; published 29 April 2013)

Temperature dependence of the x-ray absorption near-edge structure (XANES) spectra at the Pr L_3 and Tb L_3 edges was measured for the $(Pr_{1-y}Tb_y)_{0.7}Ca_{0.3}CoO_3$ system, in which a sharp spin-state (SS) transition took place at a critical temperature T_{SS}. A small increase in the valence of the terbium ion was found below T_{SS}, besides the enhancement of the praseodymium valence; the trivalent states, which are stable at room temperature, change to a $3+/4+$ ionic mixture at low temperatures. In particular for the $y = 0.2$ sample, the average valence determined at 8 K amounts to $3.25+$ and $3.03+$ for the Pr and Tb ion, respectively. In analogous $(Pr_{1-y}RE_y)_{0.7}Ca_{0.3}CoO_3$ samples (RE = Sm and Eu), in which the SS transition also took place, no valence shift of the RE ion was detected in the XANES spectra at the RE ion L_3 edge. The role of the substituted RE ion for the Pr site on the SS transition is discussed.

DOI: 10.1103/PhysRevB.87.155153 PACS number(s): 71.30.+h, 78.70.Dm, 75.30.Wx

I. INTRODUCTION

The perovskite cobaltites $RECoO_3$ (RE = rare-earth element and Y) show a spin-state (SS) transition of Co^{3+} ions from a low spin state (LS; $t_{2g}^6e_g^0$, $S = 0$) to a high spin state (HS; $t_{2g}^4e_g^2$, $S = 2$) with increasing temperature, followed by the formation of the metallic state of the intermediate spin state (IS; $t_{2g}^5\sigma^*$, $S = 1$) at higher temperatures.[1] The temperature-induced spin-state transition and its gradual course indicate a small energy difference δE between the crystal-field splitting and Hund coupling energy.[2,3] The hole-doped systems such as $La_{1-x}Sr_xCoO_3$ generally show a temperature stable phase with itinerant cobalt states (presumably the mixed IS Co^{3+}/LS Co^{4+} or HS Co^{3+}/IS Co^{4+} configurations) and undergo a ferromagnetic ordering at low temperatures. Most interestingly, some Pr-based cobaltites exhibit a pronounced first-order transition to a low-temperature phase of weakly paramagnetic character and reduced conduction. It was revealed for the first time on $Pr_{0.5}Ca_{0.5}CoO_3$ at $T_{SS} \sim 90$ K, and was documented, in addition to the steplike resistivity jump, by concomitant anomalies in the magnetic susceptibility, heat capacity, and lattice dilatation.[4,5] The change in the electronic structure was confirmed at T_{SS} by the photoemission spectroscopy.[6] The mechanism of the transition was tentatively ascribed to a spin-state crossover from the itinerant cobalt states to an ordered mixture of localized LS Co^{3+} and LS Co^{4+} ($t_{2g}^5e_g^0$, $S = 1/2$) states. Thereafter, the existence of Co^{3+}/Co^{4+} ordering was questioned because similar transition was evidenced also in the less doped $Pr_{1-x}Ca_xCoO_3$ ($x = 0.3$) under high pressures,[7] or in the $(Pr_{1-y}RE_y)_{1-x}Ca_xCoO_3$ system ($0.2 \leqslant x \leqslant 0.5$) with a partial substitution of Pr by smaller RE cations such as Sm, Eu, and Y under ambient pressure.[7–9] This transition appeared to be conditioned not only by the presence of both Pr and Ca ions, but also by a larger structural distortion of the CoO_6 network, depending on the average ionic radius and size mismatch of perovskite A-site ions.[9] Furthermore, the critical temperature T_{SS} was found to be depressed by the applied magnetic field.[10,11]

An alternative scenario explaining the nature of such specific transition was proposed on the basis of electronic structure calculations exploiting the temperature dependence of the structural experimental data for $Pr_{0.5}Ca_{0.5}CoO_3$.[12] It appeared that the formal cobalt valence should change below T_{SS} from mixed-valence $Co^{3.5+}$ towards pure $Co^{3.0+}$ with strong preference for the LS state and, concomitantly, the praseodymium valence should increase simultaneously from Pr^{3+} towards Pr^{4+}. The SS transition and electronic localization was thus intuitively interpreted as an analogy of the compositional transition from the ferromagnetic metal of $La_{0.5}Ca_{0.5}CoO_3$ to the diamagnetic insulator of $LaCoO_3$.[13,14] Shortly afterwards, the theoretical hypothesis about the crucial role of variable praseodymium valence was experimentally supported by observation of a Schottky peak in the low-temperature specific heat of $(Pr_{1-y}Y_y)_{0.7}Ca_{0.3}CoO_3$ ($y = 0.075$ and 0.15),[15] which proved a stabilization of Kramers Pr^{4+} ions in the low-temperature phase.

Recently, we directly confirmed the praseodymium valence shift, realized in fact as a mixture of the Pr^{3+} and Pr^{4+} states, from the x-ray absorption near-edge structure (XANES) spectra at the Pr L_3 edge for the same $(Pr_{1-y}Y_y)_{0.7}Ca_{0.3}CoO_3$ samples.[16] It has been found that the average valence of the praseodymium ion increases below room temperature from the common value $3.0+$, undergoes the steepest change at T_{SS}, and reaches finally $3.15+$ and $3.27+$ at 8 K for the $y = 0.075$ and 0.15 samples, respectively. Interestingly, these values are consistent with those estimated by quantitative analysis of the entropy associated with the Schottky peak dominating the low-temperature specific heat. For $Pr_{0.5}Ca_{0.5}CoO_3$, similar valence shifts from $3.0+$ at 300 K to $3.15+$ at 10 K were obtained by other authors using XANES at Pr L_3 and $M_{4,5}$ edges.[17] In addition, a change of cobalt spin states and the valence shift of the Co ion have been evidenced by the analysis of two complementary synchrotron x-ray spectroscopic techniques.[18] Very recently, the spin state of the Co^{3+} and Co^{4+} ions was estimated above and below T_{SS} by soft x-ray absorption spectroscopy at Co $L_{2,3}$ and O 1s edges in $(Pr_{0.7}Sm_{0.3})_{0.7}Ca_{0.3}CoO_3$.[19]

In the present work, we apply XANES spectroscopy measurements to the analysis of $(Pr_{1-y}RE_y)_{0.7}Ca_{0.3}CoO_3$ systems (RE = Tb, Sm, and Eu), in which the SS transition between

50–140 K was obtained.[8,9] The choice of substituting *RE* ions was motivated by the fact that terbium ion is known to adopt the mixed valence state Tb^{3+}/Tb^{4+} in several compounds.[20] The Sm and Eu ions are known to exist also in various valence states. As an example, in the Sm-based filled skutterudite, $SmOs_4Sb_{12}$, Sm ions possess a mixed valence state between Sm^{2+} and Sm^{3+}, which can be detected by XANES.[21] In the Eu-contained niobates such as $Eu_2Nb_5O_9$ and $EuNbO_3$, a mixed valence state between Eu^{2+} and Eu^{3+} was detected by photoelectron spectroscopy.[22] In the present study, we thus show a detailed temperature dependence of the XANES spectra around the *RE* L_3 edges measured using the bulk sensitive transmission method, and derive the *RE* ion states from the spectra.

II. EXPERIMENTAL

Polycrystalline samples $(Pr_{1-y}Tb_y)_{0.7}Ca_{0.3}CoO_3$ ($y = 0$, 0.1, 0.2), $(Pr_{1-y}Sm_y)_{0.7}Ca_{0.3}CoO_3$ ($y = 0.2$, 0.3, 0.4), and $(Pr_{1-y}Eu_y)_{0.7}Ca_{0.3}CoO_3$ ($y = 0.15$, 0.2, 0.3) were fabricated by a solid-state reaction. Raw powders of Pr_6O_{11}, Tb_4O_7, Sm_2O_3, Eu_2O_3, Co_3O_4, and $CaCO_3$ were weighted with proper molar ratios and ground using an agate mortar and pestle for 1 h. Mixed powders were calcined at 1000 °C for 24 h in air. Then they were pulverized, ground, and pressed into pellets of 20 mm diameter and 4 mm thickness. Pellets were sintered at 1200 °C for 24 h in 0.1 MPa flowing oxygen gas. The measured relative densities of each sample were greater than 90%. Powder x-ray diffraction patterns were taken for each sample using Cu $K\alpha$ radiation; the samples were confirmed to have a single-phase orthoperovskite *Pbnm* structure. The oxygen stoichiometry was checked on the $y = 0$ sample ($Pr_{0.7}Ca_{0.3}CoO_3$) using a high-resolution neutron diffraction, and practically ideal oxygen content 2.99 ± 0.01 has been found. For the XANES measurements, a small amount of the samples were pulverized, mixed with boron nitride powder (99.9%) with proper molar ratios in order to optimize absorption, and pelletized 6 mm in diameter and 0.5 mm in thickness.

Each XANES spectrum of the samples was measured at BL01B1 of SPring-8 in Japan. The beam was monochromatized using a Si(111) double-crystal monochromator. The spectra were recorded in the transmission mode with the detectors of the ionization chambers and obtained at various temperatures from 8 to 300 K using a cryocooler. The measurements were performed upon the heating run. The energy resolution was within 1.5 eV around $E = 8$ keV.

To determine the mixed Pr^{3+}/Pr^{4+} contents at low temperatures for $(Pr_{1-y}Tb_y)_{0.7}Ca_{0.3}CoO_3$, the calibration line was obtained using XANES spectra of Pr_6O_{11} as $Pr^{3.667+}$ and $(Pr_{1-y}Tb_y)_{0.7}Ca_{0.3}CoO_3$ as $Pr^{3.0+}$ measured at 300 K, which were performed similarly to the previous paper.[16] The recorded XANES spectra were modeled by the sum of three Lorentzian functions and one arctangent function representing the steplike edge of continuum excitations. One Lorentzian function (peak A: 5966 eV) shows an excitation from $2p_{3/2}$ to $4f^2 5d^*$, which represents $Pr^{3.0+}$ ions. The other Lorentzian functions (peak B2: 5969 eV and peak B1: 5979 eV) show the excitations from $2p_{3/2}$ to $4f^2\underline{L}5d^*$ and to $4f^1 5d^*$, $\underline{L}$ being a ligand hole in the O $2p$ orbital, both of which represent Pr^{4+} ions.[23,24] The energy differences between peaks A, B2, and B1 were fixed according to results of Hu *et al.*[25] The curve fittings were performed in the energy range from 5944 to 5985 eV using ATHENA software.[26]

To estimate the mixed Tb^{3+}/Tb^{4+} contents, a similar procedure was applied. A comparative measurement of Tb_4O_7 and $(Pr_{1-y}Tb_y)_{0.7}Ca_{0.3}CoO_3$ was carried out at 300 K as standards of $Tb^{3.5+}$ and $Tb^{3.0+}$, respectively. The recorded XANES spectra for Tb L_3 line were modeled by the sum of two Lorentzian functions [peak C: 7518 eV for Tb^{3+} ($4f^8$) and peak D: 7528 eV for Tb^{4+} ($4f^7$)] and one arctangent function. For simplicity, the peak related to the ligand hole state $4f^8\underline{L}$ was omitted because of its weaker intensity as reported by Dexpert *et al.*[27] For $(Pr_{0.7}Sm_{0.3})_{0.7}Ca_{0.3}CoO_3$, and $(Pr_{0.85}Eu_{0.15})_{0.7}Ca_{0.3}CoO_3$ samples, the XANES spectra were measured around Pr L_3 (5966 eV), Sm L_3 (6720 eV), and Eu L_3 (6981 eV) edges, respectively.

Electrical resistivity $\rho(T)$ was measured on the heating run using a four-probe method with a parallelepiped sample cut from the pellet with a typical current density of 0.01 A/cm^2. Magnetic susceptibility $\chi(T)$ was measured under the magnetic field of 0.1 T after field cooling using a superconducting quantum interference device (SQUID) magnetometer (Quantum Design MPMS-XL).

III. RESULTS AND DISCUSSION

A. Magnetic and electrical properties in $(Pr_{1-y}Tb_y)_{0.7}Ca_{0.3}CoO_3$

The magnetic susceptibility $\chi(T)$ of the $(Pr_{1-y}Tb_y)_{0.7}Ca_{0.3}CoO_3$ ($y = 0$, 0.1, 0.2) samples is presented in Fig. 1(a). For the Tb free sample $y = 0$, $\chi(T)$ steeply increases to large values at low temperatures in accordance with the ferromagnetic ground state of this compound ($T_C \sim 55$ K). The Tb-substituted samples exhibit a marked drop of magnetic susceptibility, which is a strong sign that cobalt ions transform to LS states at low temperature. A sharp transition can be seen at 75 K for the $y = 0.1$ sample. For the $y = 0.2$ sample, a broad transition was observed at 145 K. These characteristics of the Tb-substituted samples are the same as those observed for $(Pr_{1-y}Y_y)_{0.7}Ca_{0.3}CoO_3$ and other $(Pr_{1-y}RE_y)_{0.7}Ca_{0.3}CoO_3$ systems.[8,9] It is worth mentioning that, in distinction to Y and Sm substituted samples, the low-temperature susceptibility increases with y, which should be related to large moment of Tb ion independently on its trivalent or tetravalent state. (Tb^{3+} with $4f^8$ configuration is a specific case of non-Kramers ion. Although its eigenstates are nonmagnetic in the low-symmetry crystal field of *Pbnm* perovskite structure, the ground and first excited singlets are nearly degenerate, forming a magnetic quasidoublet.[28])

The electrical resistivity $\rho(T)$ of the same samples is presented in Fig. 1(b). The resistivity measured on the $y = 0$ sample is only weakly temperature dependent, without any sign of phase transition below 300 K. On the other hand, the Tb-substituted samples show features typical for the conductivity change similarly to $Pr_{0.5}Ca_{0.5}CoO_3$.

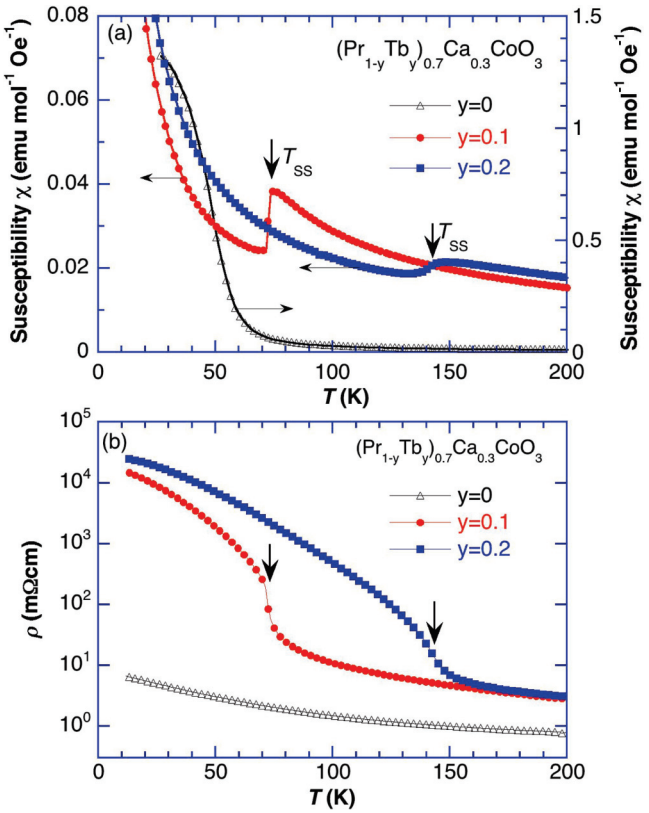

FIG. 1. (Color online) Temperature dependence of the (a) magnetic susceptibility $\chi(T)$ and (b) electrical resistivity $\rho(T)$ for the $(Pr_{1-y}Tb_y)_{0.7}Ca_{0.3}CoO_3$ samples ($y = 0$, 0.1, and 0.2). The measurements were performed on the heating runs.

B. XANES measurements of Pr L_3 and Tb L_3 edges

Figure 2(a) shows the temperature dependence of the XANES spectra at the Pr $L3$ edge for the $(Pr_{0.8}Tb_{0.2})_{0.7}Ca_{0.3}CoO_3$ sample. Two main peaks situated at 5966 and 5979 eV (named peaks A and B1) originate from the Pr $2p \rightarrow 5d$ transitions. At 300 K, the Pr^{3+} ($4f^2$) sites essentially contribute to the peak A, with a little component at peak B2, which is caused presumably by multiple scattering, commonly treated in the theoretical simulations of XANES.[16] At temperatures close to $T_{SS} \sim 145$ K, the shape of the XANES spectra changes markedly; the intensity of peak B1 increases notably and shifts to lower energy side, while the intensity of peak A decreases. At the same time, a new component (peak B2 at 5969 eV) can be resolved on its high-energy slope. Since the B1 and B2 peaks are manifestations of Pr^{4+} states, originating in particular of the configurations $4f^1$ and $4f^2\underline{L}$,[23–25] the observed changes confirm that the average valence of the Pr ions in the $(Pr_{1-y}Tb_y)_{0.7}Ca_{0.3}CoO_3$ increases from 3+ toward 4+ below T_{SS}, consistently with those reported for $(Pr_{1-y}Y_y)_{0.7}Ca_{0.3}CoO_3$ by us[16] or for $Pr_{0.5}Ca_{0.5}CoO_3$ by García-Muñoz *et al.*[17] In Fig. 2(a), the first oscillation around 6000 eV can be seen in the XANES spectra, where the broad peak shifts to the high-energy side with decreasing temperature. These results qualitatively suggest that the Pr-O distance shortens with decreasing temperature. The detailed analysis must be performed using extended x-ray absorption fine structure (EXAFS).

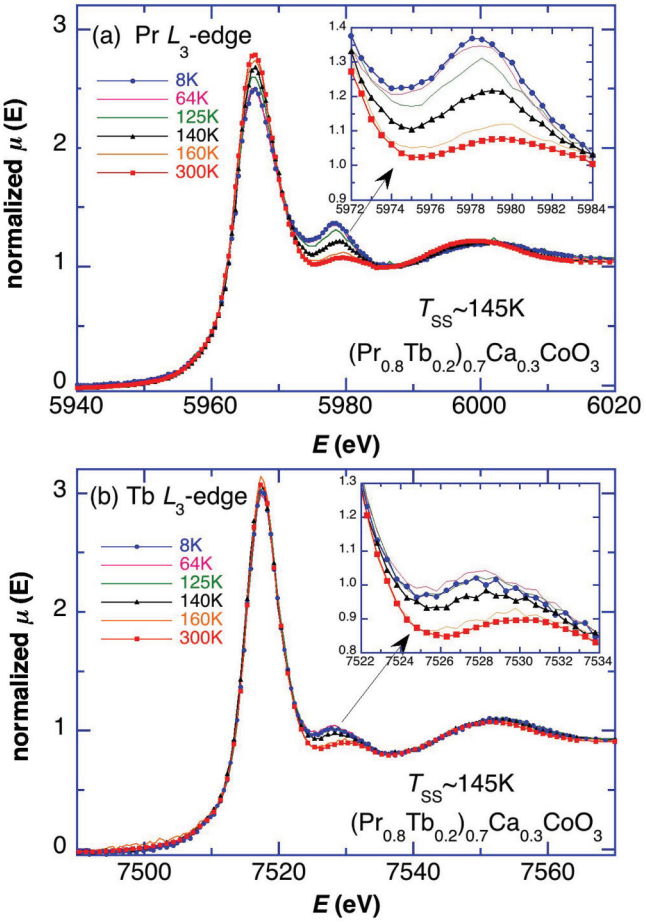

FIG. 2. (Color online) Temperature dependence of the XANES spectra at the (a) Pr L_3 edge and (b) Tb L_3 edge for the $(Pr_{0.8}Tb_{0.2})_{0.7}Ca_{0.3}CoO_3$ sample. Insets show the magnification around the $4f^1$ and $4f^7$ spectra related with the Pr^{4+} and Tb^{4+} ions, respectively.

Figure 2(b) shows the temperature dependence of the XANES spectra at the Tb L_3 edge for the same $(Pr_{0.8}Tb_{0.2})_{0.7}Ca_{0.3}CoO_3$ sample. Two main peaks situated at 7518 and 7529 eV (named peaks C and D) originate from the Tb $2p \rightarrow 5d$ transitions. The spectrum at 300 K is characteristic for the Tb^{3+} ($4f^8$) valence, contributing to the main peak C. The form of XANES spectra is changing around $T_{SS} \sim 145$ K. There is a small drop of the intensity of peak C, which is a fingerprint of Tb^{3+}, and at the same time, peak D increases slightly and shifts to lower energy. The peak D is a manifestation of Tb^{4+} states, namely, of the configuration $4f^7$.[27,29] The observed behavior thus suggests that the valence of the Tb ions increases below T_{SS}, simultaneously with the valence shift of Pr ions. In Fig. 2(b), a slight peak shift of the first oscillation around 7552 eV can be also observed with decreasing temperature.

C. Valence shifts of the Pr and Tb ions

In order to determine the valence shift of Pr ion quantitatively, the XANES spectra were fitted to a sum of three Lorentzian functions (peak A for Pr^{3+} and peaks B1 and B2 for Pr^{4+}) and one arctangent function, as indicated in Ref. 16.

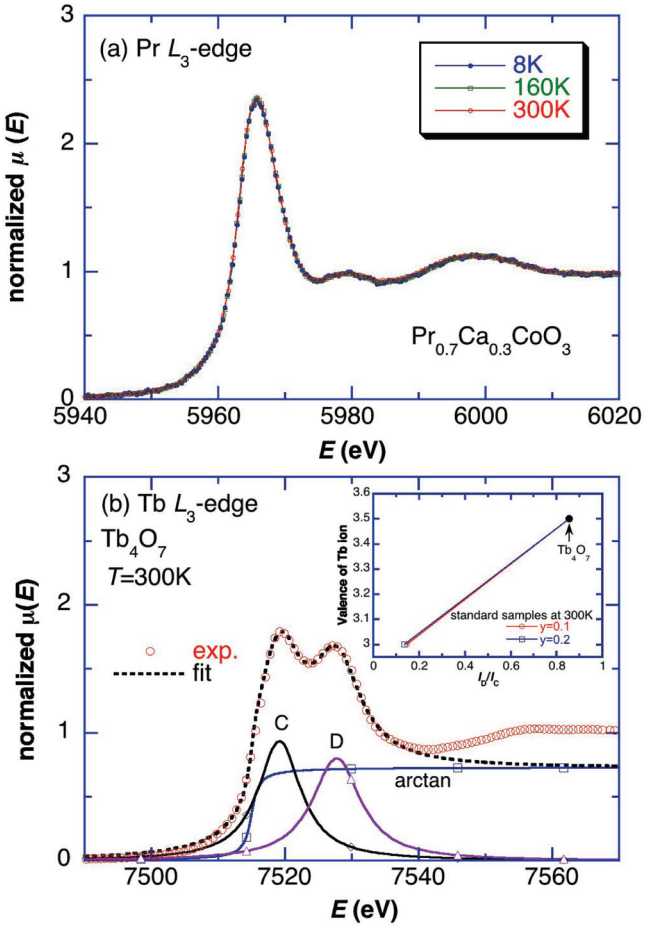

FIG. 3. (Color online) (a) Temperature dependence of the XANES spectra at the Pr L_3 edge for $Pr_{0.7}Ca_{0.3}CoO_3$. (b) The XANES spectrum for Tb_4O_7 at 300 K, fitted by a sum of two Lorentzian functions (peak C for Tb^{3+} and peak D for Tb^{4+}) and one arctangent function. The inset shows the calibration lines to determine the valence of the Tb ion in the $(Pr_{1-y}Tb_y)_{0.7}Ca_{0.3}CoO_3$ samples ($y = 0.1, 0.2$).

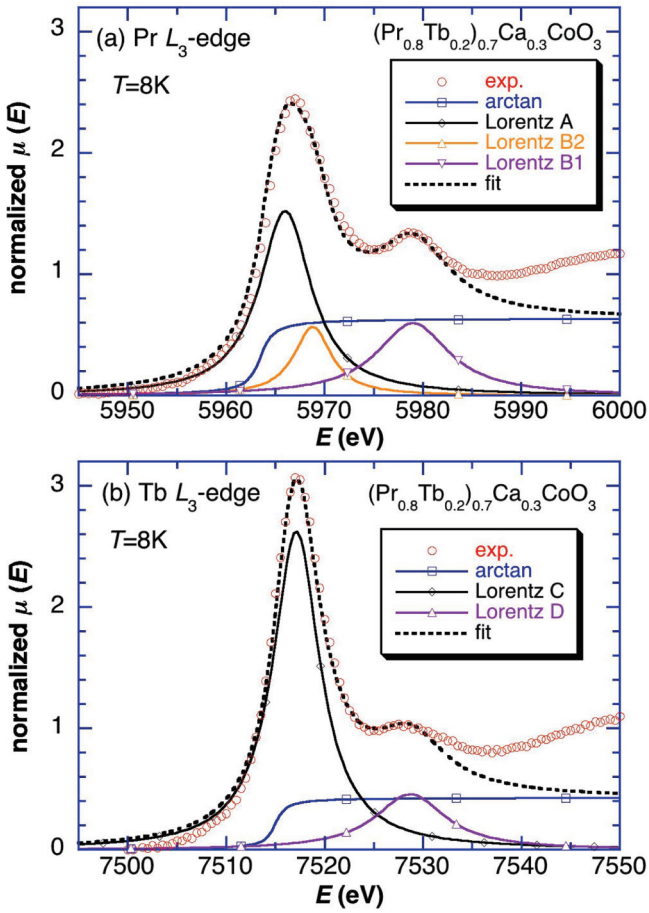

FIG. 4. (Color online) Examples of the fitting of the XANES spectrum at the (a) Pr L_3 and (b) Tb L_3 edge for the $(Pr_{0.8}Tb_{0.2})_{0.7}Ca_{0.3}CoO_3$ sample at 8 K. For the fitting of the Pr L_3 edge, one arctangent function and three Lorentzian functions (A, B1, and B2) are used. For the fitting of the Tb L_3 edge, one arctangent function and two Lorentzian functions (C and D) are used.

Then the valence of Pr ions in the Tb-substituted samples was deduced from the intensity ratio I_{B1}/I_A of the B1 spectral peak to the A spectral peak using the calibration line that took into account the actual I_{B1}/I_A values for $Pr^{3.0+}$ and that for $Pr^{3.667+}$ (not shown). Figure 3(a) shows the temperature dependence of the XANES spectra at the Pr L_3 edge for pure $Pr_{0.7}Ca_{0.3}CoO_3$ with ferromagnetic metallic ground state (see Fig. 1). Apart of the main peak A, there is again a small bump at around 5980 eV, originating in the multiple scattering as mentioned above. The same feature has been observed for another metallic compound $Pr_{0.55}Ca_{0.45}CoO_3$,[17] and seems thus to be a general manifestation of trivalent praseodymium in the mixed Co^{3+}/Co^{4+} systems. Importantly, no spectral change of the Pr L_3 edge is observed down to 8 K, which suggests that the Pr^{3+} valence in $Pr_{0.7}Ca_{0.3}CoO_3$ remains temperature independent.

Figure 3(b) shows the XANES spectrum for Tb_4O_7 at 300 K, which was fitted to a sum of two Lorentzian functions (peak C for Tb^{3+} and peak D for Tb^{4+}) and one arctangent function. The measurement was also performed down to low temperatures and since no relevant spectroscopic changes were detected, the spectrum, in particular the intensity ratio I_D/I_C, was further considered as a standard for $Tb^{3.5+}$. The valence of Tb ions in the $(Pr_{1-y}Tb_y)_{0.7}Ca_{0.3}CoO_3$ samples was simply deduced from observed intensity ratio I_D/I_C of the D to C spectral peaks,[23] taking the data at 300 K as a standard of $Tb^{3.0+}$. This has been done with use of the calibration line in the inset of Fig. 3(b); $I_D/I_C = 0.856$ for $Tb^{3.5+}$ in Tb_4O_7 and $I_D/I_C = 0.136$ for $Tb^{3.0+}$ in $(Pr_{0.8}Tb_{0.2})_{0.7}Ca_{0.3}CoO_3$.

The fit of XANES spectra is exemplified in Fig. 4(a) using the data for the $(Pr_{0.8}Tb_{0.2})_{0.7}Ca_{0.3}CoO_3$ sample at 8 K, where the valence change achieves a maximum. It turns out that the XANES spectrum at Pr L_3 edge is well reproduced within the energy range from 5944 to 5985 eV including the peaks related to Pr^{3+} and Pr^{4+}. The B2 component at the slope of main peak A is also resolved and the presence of Pr^{3+}/Pr^{4+} mixture is thus obvious. Figure 4(b) shows the fit of the XANES spectrum at Tb L_3 edge for the same sample, also at 8 K. The XANES spectrum cannot be reproduced without considering both characteristic peaks of Tb^{3+} and Tb^{4+} (features C and D, respectively).

The results based on the curve fitting of XANES spectra are summarized in Figs. 5(a) and 5(b), which show, respectively,

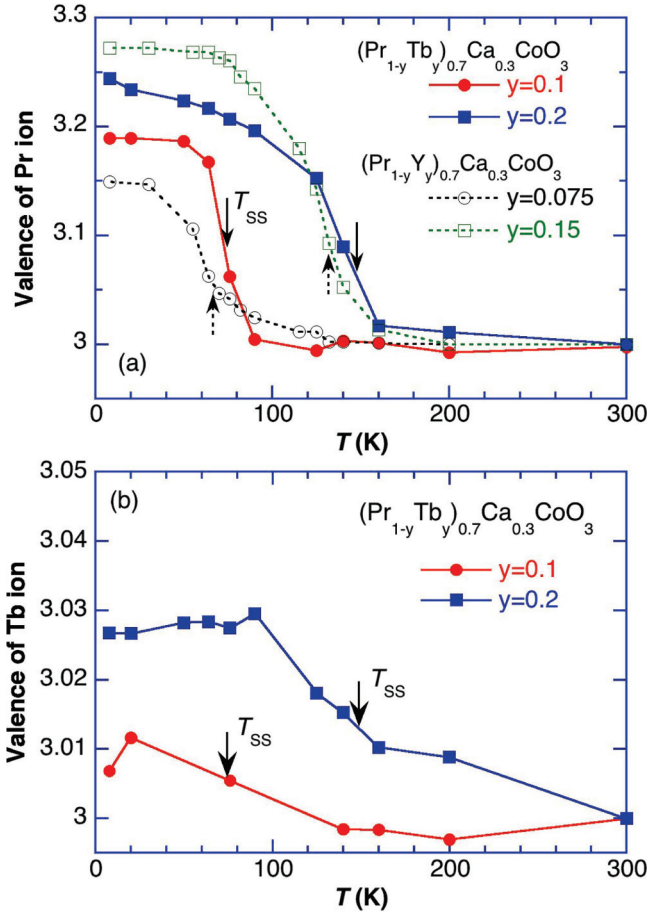

FIG. 5. (Color online) Temperature dependence of the average valence of (a) Pr ion and (b) Tb ion for the $(Pr_{1-y}Tb_y)_{0.7}Ca_{0.3}CoO_3$ samples estimated using the XANES spectra and curve fitting. In (a), the estimated valence of Pr ion for the reported $(Pr_{1-y}Y_y)_{0.7}Ca_{0.3}CoO_3$ samples ($y = 0.075$ and 0.15; Ref. 16) is also presented. The uncertainty of the estimated valence values is within 1% of the absolute value.

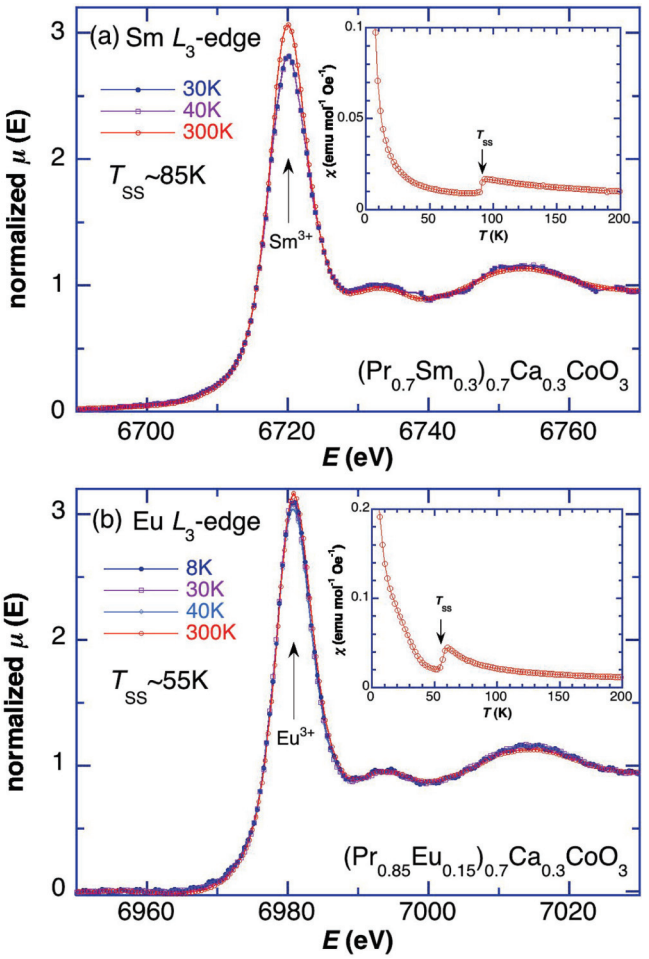

FIG. 6. (Color online) Temperature dependence of the XANES spectra at (a) Sm L_3 edge for $(Pr_{0.7}Sm_{0.3})_{0.7}Ca_{0.3}CoO_3$ and (b) Eu L_3 edge for $(Pr_{0.85}Eu_{0.15})_{0.7}Ca_{0.3}CoO_3$ samples. Inset shows the magnetic susceptibility $\chi(T)$ of each sample.

the temperature dependence of the valence of Pr and Tb ions in the $(Pr_{1-y}Tb_y)_{0.7}Ca_{0.3}CoO_3$ samples. Contrary to the sharp SS transitions detected by the magnetic susceptibility and electric resistivity, the average Pr valence changes on cooling from 300 K gradually, though with the steepest increase at T_{SS}. Finally at the lowest temperatures, the valence reaches final values of 3.19+ and 3.25+ for the $y = 0.1$ and 0.2 samples, respectively. The uncertainty of the estimated valence values is within 1% of the absolute value, which arises from the arbitrariness of parameters used in the arctangent and Lorentzian functions. Comparing the results for $(Pr_{1-y}Tb_y)_{0.7}Ca_{0.3}CoO_3$ and those for the $(Pr_{1-y}Y_y)_{0.7}Ca_{0.3}CoO_3$ samples ($y = 0.075$ and 0.15)[16] also presented in Fig. 5(a), one finds that the enhancement of the Pr valence systematically increases with increasing contents of the substitution with smaller Tb or Y ions, i.e., with decreasing of the mean size of the A-site cation in the perovskite structure.

As the Tb valence in $(Pr_{1-y}Tb_y)_{0.7}Ca_{0.3}CoO_3$ is concerned, it changes gradually around T_{SS} and reaches final values of 3.01+ and 3.03+ at 8 K for the $y = 0.1$ and 0.2 samples, respectively [see Fig. 5(b)]. We note, however, that the increase in the Tb valence is about one order of magnitude smaller and its "gradual" character is even more pronounced than in the case of Pr valence.

D. XANES measurements at *RE* edges for $(Pr_{1-y}RE_y)_{0.7}Ca_{0.3}CoO_3$ (*RE* = Sm, Eu)

To illustrate the valence states of the substituted Sm and Eu ions in $(Pr_{1-y}RE_y)_{0.7}Ca_{0.3}CoO_3$, the temperature-dependent XANES spectra at the Sm L_3 edge and Eu L_3 edge are compiled in Figs. 6(a) and 6(b). The insets present the data on magnetic susceptibility $\chi(T)$ on the heating run, which demonstrate the transition at 85 K and 55 K for the $RE = Sm$ ($y = 0.3$) and Eu ($y = 0.15$) samples, respectively.

For the samarium-substituted sample, although the intensity of the main peak of Sm^{3+} at 6720 eV slightly decreased with decreasing T, no isomeric shift or new spectral feature is detected. This result suggests that the Sm valence remains essentially as 3.0+ over the entire temperature range. For the europium-substituted sample, the spectrum does not change at all down to 8 K and, consequently, the valence of the Eu ion also remains 3.0+. Let us note that properties of the Sm-doped system became a subject of very recent paper by Guillou *et al.*[19]

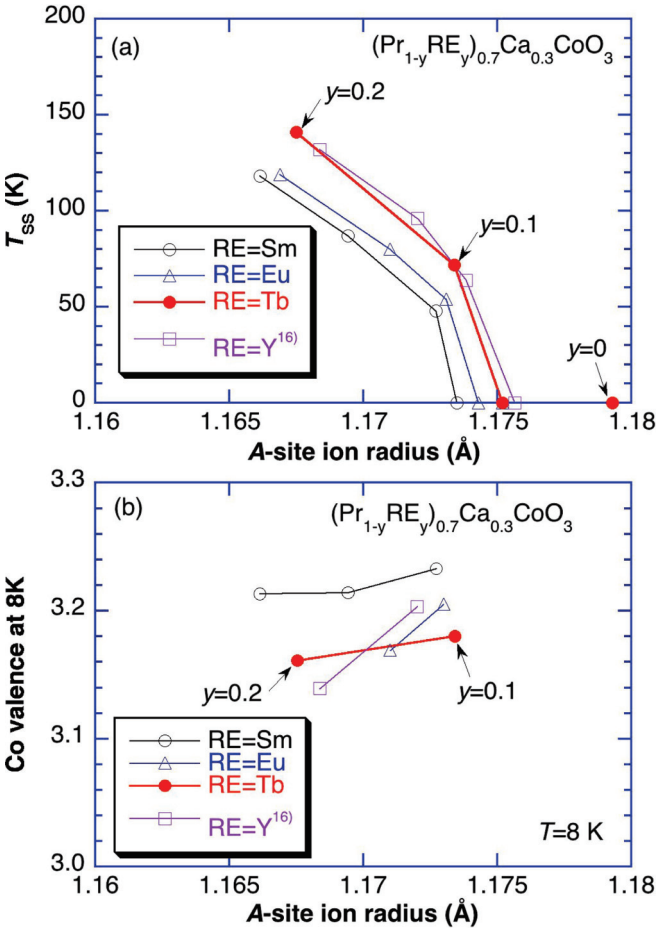

FIG. 7. (Color online) (a) The transition temperature T_{SS} and (b) the calculated valence of Co ion at 8 K, as a function of the average ionic radius of the perovskite A site, $\langle r_A \rangle$, for various $(Pr_{1-y}RE_y)_{0.7}Ca_{0.3}CoO_3$ systems. The results for the RE = Y were cited from Ref. 16. In (b), the uncertainty of the estimated valence values is within 1% of the absolute value.

E. Discussion

The unusual SS transition occurring in some Pr-based cobaltites is intimately connected with a charge transfer between praseodymium and cobalt sites. Such process is enabled by energy closeness of the Pr^{3+}/Pr^{4+} valence states. In the previous subsections, a possibility of more complex valence equilibria has been probed on $(Pr_{1-y}RE_y)_{0.7}Ca_{0.3}CoO_3$ systems with the RE = Tb, Sm, Eu substitutions at Pr sites, in which mixed valence states, RE^{3+}/RE^{4+} or RE^{3+}/RE^{2+}, can eventually also occur. Indeed, a small but unquestionable increase in the valence of RE ion is observed for the Tb-substituted samples below T_{SS}, besides the substantial enhancement of the Pr ion valence to 3.25+. On the other hand, no temperature variation of the Sm and Eu valence state is detected for such RE-substituted samples. This means that hypothetical redox reaction between rare-earth elements, such as $Pr^{3+}+Sm^{3+} \rightarrow Pr^{4+}+Sm^{2+}$, does not play any role both above and below the MI transition.

To demonstrate the effect of particular rare-earth elements, the transition temperature T_{SS} is plotted in Fig. 7(a) as a function of the average ionic radius of the perovskite A site, $\langle r_A \rangle$. The experimental results for the RE = Y system (y = 0.075, 0.1, and 0.2) are also shown.[16] It is seen that the interrelation between T_{SS} and $\langle r_A \rangle$ is not universal; the curves gradually shift to the large-$\langle r_A \rangle$ side with decreasing ionic radius of RE. In this comparison, the curve for RE = Tb is not peculiar, which can be understood, since the actual shift of Tb valence is fairly small (to 3.03+ in maximum). Nonetheless, the possibility of Tb^{3+}/Tb^{4+} crossover in cobaltites is confirmed and additional studies aiming to exemplify this valence change are under way. As a final note to Fig. 7(a) we may mention that the T_{SS} vs $\langle r_A \rangle$ relation is applicable only for the $(Pr_{1-y}RE_y)_{0.7}Ca_{0.3}CoO_3$ systems and does not hold for the intensively studied system $Pr_{0.5}Ca_{0.5}CoO_{3-\delta}$, in which the Co, Pr valences and T_{SS} strongly depend on the actual oxygen content.[4,7,17,30,31]

Finally, in Fig. 7(b) we plot the formal valence of Co ions in the $(Pr_{1-y}RE_y)_{0.7}Ca_{0.3}CoO_3$ at 8 K as a function of $\langle r_A \rangle$, calculated based on the Pr or Tb valences estimated from XANES data. This is enabled by the fact that, unlike $Pr_{0.5}Ca_{0.5}CoO_{3-\delta}$, the $Pr_{0.7}Ca_{0.3}CoO_3$ derived systems are prepared generally as stoichiometric ones, as proved for selected samples by thermogravimetry or neutron diffraction method. The oxygen stoichiometry can be inferred also indirectly, comparing the electric transport properties, as shown in our previous paper on the Y-substituted samples.[15] The results in Fig. 7(b) show that the doping level of the cobalt subsystem decreases from 0.30 hole per f.u. to about 0.15 hole per f.u., similar for Tb content of y = 0.1 and 0.2. Analogous data for other RE system studied by us are also presented.

IV. CONCLUSION

Temperature dependence of the x-ray absorption near-edge structure (XANES) spectra at the Pr L_3 and RE L_3 edges was measured for the $(Pr_{1-y}RE_y)_{0.7}Ca_{0.3}CoO_3$ samples (RE = Tb, Sm, and Eu), in which a spin-state (SS) transition took place at a critical temperature T_{SS}. The important experimental results and conclusions are summarized as follows.

(1) In all the studied Pr-based cobaltites, the trivalent praseodymium ions change to a Pr^{3+}/Pr^{4+} mixture below T_{SS}, which anticipates that, at the same time, the formal cobalt valence should decrease from 3.3+ closer to 3.0+.

(2) Besides the enhancement of the Pr valence, a small increase in the valence of the Tb ion is found in the $(Pr_{1-y}Tb_y)_{0.7}Ca_{0.3}CoO_3$ samples below T_{SS}. In the y = 0.2 sample, the average valence determined at 8 K makes 3.25+ and 3.03+ for the Pr and Tb ion, respectively. The calculated Co valence is 3.156+ in this case. It should be noted that these results do not necessarily mean very different tendencies of the two rare-earth ions for tetravalent states, since the final valence balance in such chemically inhomogeneous systems depends also on steric factors, including the size mismatch at perovskite A sites.

(3) The observed valence shift of Tb ion indicates the energy closeness of trivalent and tetravalent states in this rare-earth element. This fact suggests that the unusual SS transition need

not be unique for the Pr-based cobaltites but can be expected also for the Tb-based ones.

(4) In the $(Pr_{1-y}RE_y)_{0.7}Ca_{0.3}CoO_3$ samples (RE = Sm and Eu) with similar transition, no valence shift of the RE ion is detected at the RE ion absorption edge in the XANES spectra. This suggests that Eu^{3+} and Sm^{3+} are stable in the system over the entire temperature range, and may signify that the energy closeness of trivalent and divalent states in these rare-earth elements has no effect on the praseodymium/cobalt valence equilibria.

ACKNOWLEDGMENTS

The synchrotron radiation experiments were performed at the BL01B1 of SPring-8 with approval of Japan Synchrotron Radiation Research Institute (JASRI) (Proposals No. 2011A1060, No. 2011B1075, and No. 2012A1118). Part of the work was performed under the financial support of a Grant-in-Aid for Scientific Research (No. 24540355) from the Ministry of Education, Culture, Sports, Science, and Technology, Japan, and the Grant Agency of the Czech Republic within the Project No. 204/11/0713.

[1] Z. Jirák, J. Hejtmánek, K. Knížek, and M. Veverka, Phys. Rev. B **78**, 014432 (2008).
[2] M. A. Korotin, S. Yu. Ezhov, I. V. Solovyev, V. I. Anisimov, D. I. Khomskii, and G. A. Sawatzky, Phys. Rev. B **54**, 5309 (1996).
[3] J.-Q. Yan, J.-S. Zhou, and J. B. Goodenough, Phys. Rev. B **69**, 134409 (2004).
[4] S. Tsubouchi, T. Kyômen, M. Itoh, P. Ganguly, M. Oguni, Y. Shimojo, Y. Morii, and Y. Ishii, Phys. Rev. B **66**, 052418 (2002).
[5] S. Tsubouchi, T. Kyômen, M. Itoh, and M. Oguni, Phys. Rev. B **69**, 144406 (2004).
[6] T. Saitoh, Y. Yamashita, N. Todoroki, T. Kyomen, M. Itoh, M. Higashiguchi, M. Nakatake, and K. Shimada, J. Electron Spectrosc. Relat. Phenom. **144–147**, 893 (2005).
[7] T. Fujita, T. Miyashita, Y. Yasui, Y. Kobayashi, M. Sato, E. Nishibori, M. Sakata, Y. Shimojo, N. Igawa, Y. Ishii, K. Kakurai, T. Adachi, Y. Ohishi, and M. Takata, J. Phys. Soc. Jpn. **73**, 1987 (2004).
[8] T. Fujita, S. Kawabata, M. Sato, N. Kurita, M. Hedo, and Y. Uwatoko, J. Phys. Soc. Jpn. **74**, 2294 (2005).
[9] T. Naito, H. Sasaki, and H. Fujishiro, J. Phys. Soc. Jpn. **79**, 034710 (2010).
[10] M. Maryško, Z. Jirák, K. Knížek, P. Novák, J. Hejtmánek, T. Naito, H. Sasaki, and H. Fujishiro, J. Appl. Phys. **109**, 07E127 (2011).
[11] T. Naito (unpublished).
[12] K. Knížek, J. Hejtmánek, P. Novák, and Z. Jirák, Phys. Rev. B **81**, 155113 (2010).
[13] J. Wu and C. Leighton, Phys. Rev. B **67**, 174408 (2003).
[14] K. Knížek, Z. Jirák, J. Hejtmánek, and P. Novák, J. Magn. Magn. Mater. **322**, 1221 (2010).
[15] J. Hejtmánek, E. Šantavá, K. Knížek, M. Maryško, Z. Jirák, T. Naito, H. Sasaki, and H. Fujishiro, Phys. Rev. B **82**, 165107 (2010).
[16] H. Fujishiro, T. Naito, S. Ogawa, N. Yoshida, K. Nitta, J. Hejtmánek, K. Knížek, and Z. Jirák, J. Phys. Soc. Jpn. **81**, 064079 (2012).
[17] J. L. García-Muñoz, C. Frontera, A. J. Barón-González, S. Valencia, J. Blasco, R. Feyerherm, E. Dudzik, R. Abrudan, and F. Radu, Phys. Rev. B **84**, 045104 (2011); J. Herrero-Martín, J. L. García-Muñoz, S. Valencia, C. Frontera, J. Blasco, A. J. Barón-González, G. Subías, R. Abrudan, F. Radu, E. Dudzik, and R. Feyerherm, *ibid.* **84**, 115131 (2011).
[18] J. Herrero-Martín, J. L. García-Muñoz, K. Kvashnina, E. Gallo, G. Subías, J. A. Alonso, and A. J. Barón-González, Phys. Rev. B **86**, 125106 (2012).
[19] F. Guillou, Q. Zhang, Z. Hu, C. Y. Kuo, Y. Y. Chin, H. J. Lin, C. T. Chen, A. Tanaka, L. H. Tjeng, and V. Hardy, Phys. Rev. B **87**, 115114 (2013).
[20] E. Largeau, M. El-Ghozzi, and D. Avignant, J. Solid State Chem. **139**, 248 (1998).
[21] M. Mizumaki, S. Tsutsui, H. Tanida, T. Uruga, D. Kikuchi, H. Sugawara, and H. Sato, J. Phys. Soc. Jpn. **76**, 053706 (2007).
[22] C. Felser, J. Kohler, A. Simon, O. Jepson, G. Svensson, S. Cramm, and W. Eberhardt, Phys. Rev. B **57**, 1510 (1998).
[23] H. Yamaoka, H. Oohashi, I. Jarrige, T. Terashima, Y. Zou, H. Mizota, S. Sakakura, T. Tochio, Y. Ito, E. Ya. Sherman, and A. Kotani, Phys. Rev. B **77**, 045135 (2008).
[24] A. Bianconi, A. Marcelli, H. Dexpert, R. Karnatak, A. Kotani, T. Jo, and J. Petiau, Phys. Rev. B **35**, 806 (1987).
[25] Z. Hu, S. Bertram, and G. Kaindl, Phys. Rev. B **49**, 39 (1994).
[26] B. Ravel and M. Newville, J. Synchrotron Rad. **12**, 537 (2005).
[27] H. Dexpert, R. C. Karnatak, J. M. Esteva, J. P. Connerade, M. Gasgnier, P. E. Caro, and L. Albert, Phys. Rev. B **36**, 1750 (1987).
[28] J. B. Gruber, K. L. Nash, R. M. Yow, D. K. Sardar, U. V. Valiev, A. A. Uzokov, and G. W. Burdick, J. Lumin. **128**, 1271 (2008).
[29] G. Kalkowski, G. Kaindl, G. Wortmann, D. Lentz, and S. Krause, Phys. Rev. B **37**, 1376 (1988).
[30] P. Tong, Y. Wu, B. Kim, D. Kwon, J. M. S. Park, and B. G. Kim, J. Phys. Soc. Jpn. **78**, 034702 (2009).
[31] A. Chichev, M. Dlouhá, S. Vratislav, J. Hejtmánek, Z. Jirák, K. Knížek, and M. Maryško, Z. Kristallogr. Suppl. **26**, 435 (2007).